Supplemental Materials

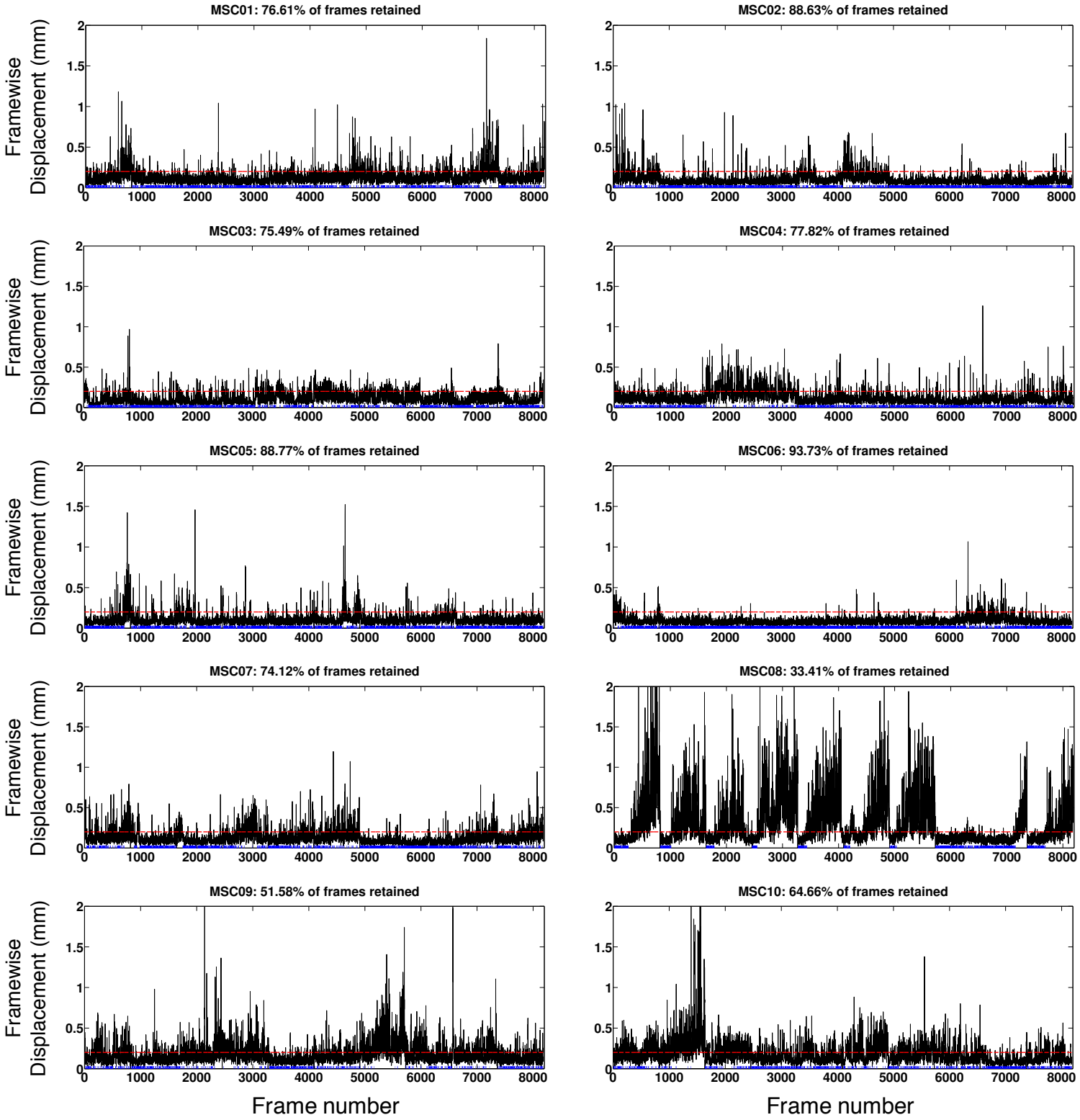

Figure S1. Related to STAR Methods – Quantification and Statistical Analysis – RSFC preprocessing. Motion estimates across runs for each of ten subjects. The black trace indicates the framewise displacement (total motion relative to previous frame). The dotted red line indicates the threshold for frame exclusion. Blue dots on the x-axis indicate retained frames.

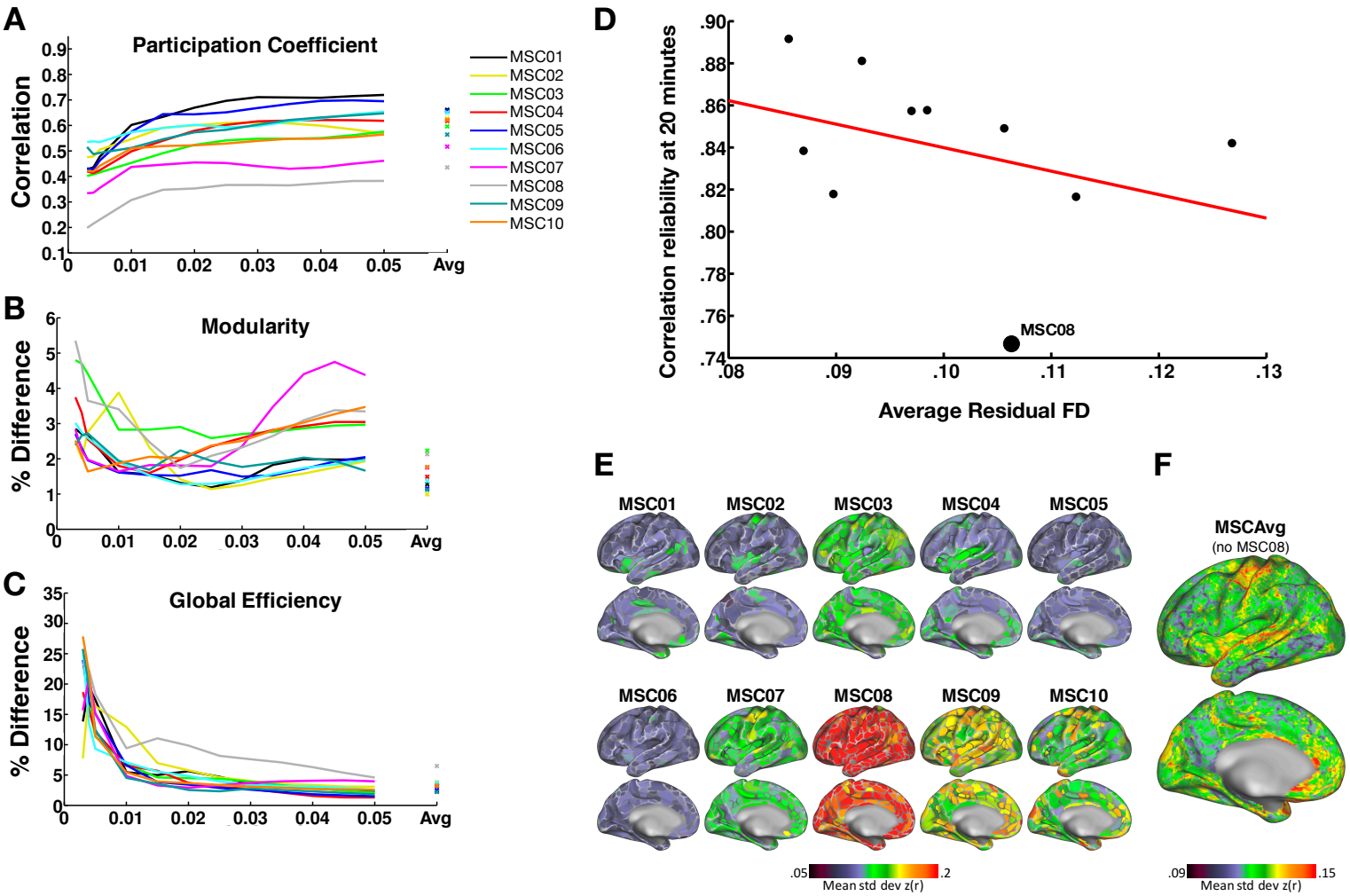

Figure S2. Related to Figure 2. A-C: Graph metric reliability dependence on graph density. The plotted values were computed using the maximum quantity of uncensored data (up to 100 minutes) represented in Fig. 2. The reliabilities of cross-threshold average metrics calculated in this quantity of data are plotted as 'x's on the right. **A**: Participation Coefficient reliability increases with density up to ~1-2% density, then levels off. **B:** Modularity is relatively unstable except in a narrow range of densities centered on 0.025. **C:** Global Efficiency reliability systematically increases with increasing graph density. **D:** Relationships between residual motion in each subject (average framewise displacement [FD] across frames retained after motion censoring) and reliability of RSFC matrices calculated from 20 minutes of data. Residual FD (nonsignificantly) predicts reliability, r=-.35, p=.31. Subject MSC08 is very far below the fit line, indicating that the low data reliability in this subject is driven by other factors beyond residual motion. **E,F:** Regional differences in within-individual variance in RSFC measures. **E:** For each parcel in each subject, the standard deviation (across sessions) of RSFC strength (Z-transformed r-values), averaged across all connections to that parcel. **F:** Mean standard deviations averaged across all subjects except MSC08, excluding zero-values in border vertices.

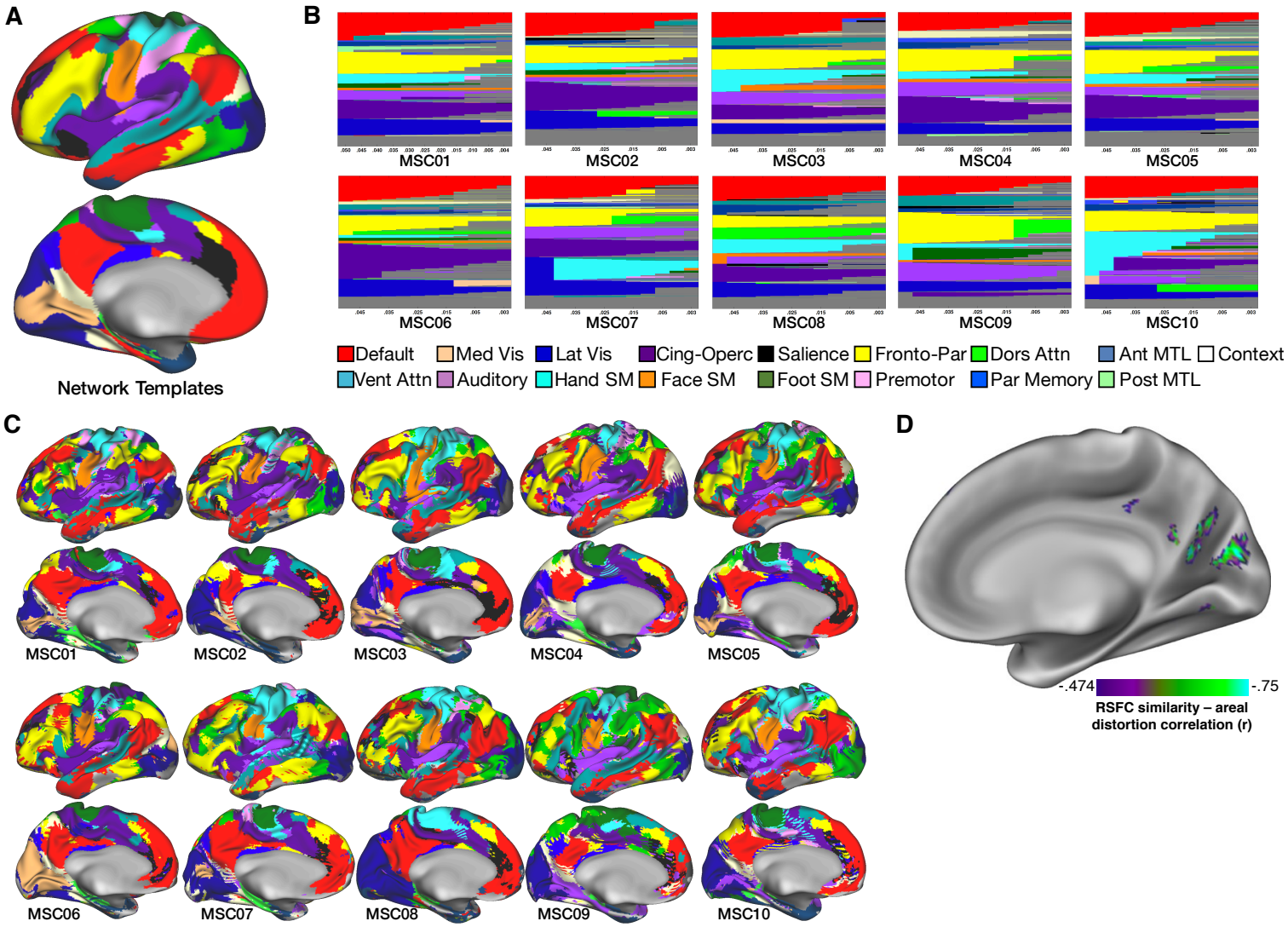

Figure S3. Related to Figure 3: A: Network templates derived from an independent dataset that were used to identify networks in the present subjects. **B**: Networks present across density thresholds in each subject. **C:** Uncertainty of network assignments. Regions of uncertain assignment (identified as regions which changed assignment across density thresholds) are striped with multiple colors representing the multiple possible assignments. **D:** Negative vertexwise associations between similarities of whole-brain RSFC patterns (computed pairwise between subjects) and differences in areal distortion (calculated pairwise between subjects). Correlations shown here are significant after permutation-based cluster correction, which established a joint height threshold of $|r|>.474$ (corresponding to $p<.001$ uncorrected) and cluster extent threshold of 25 mm2. This corresponded to an overall corrected level of $p<.05$. This finding indicates that in and near parieto-occipital sulcus, inter-subject variability in RSFC patterns was affected by anatomical differences in the shape of the cortical surface.

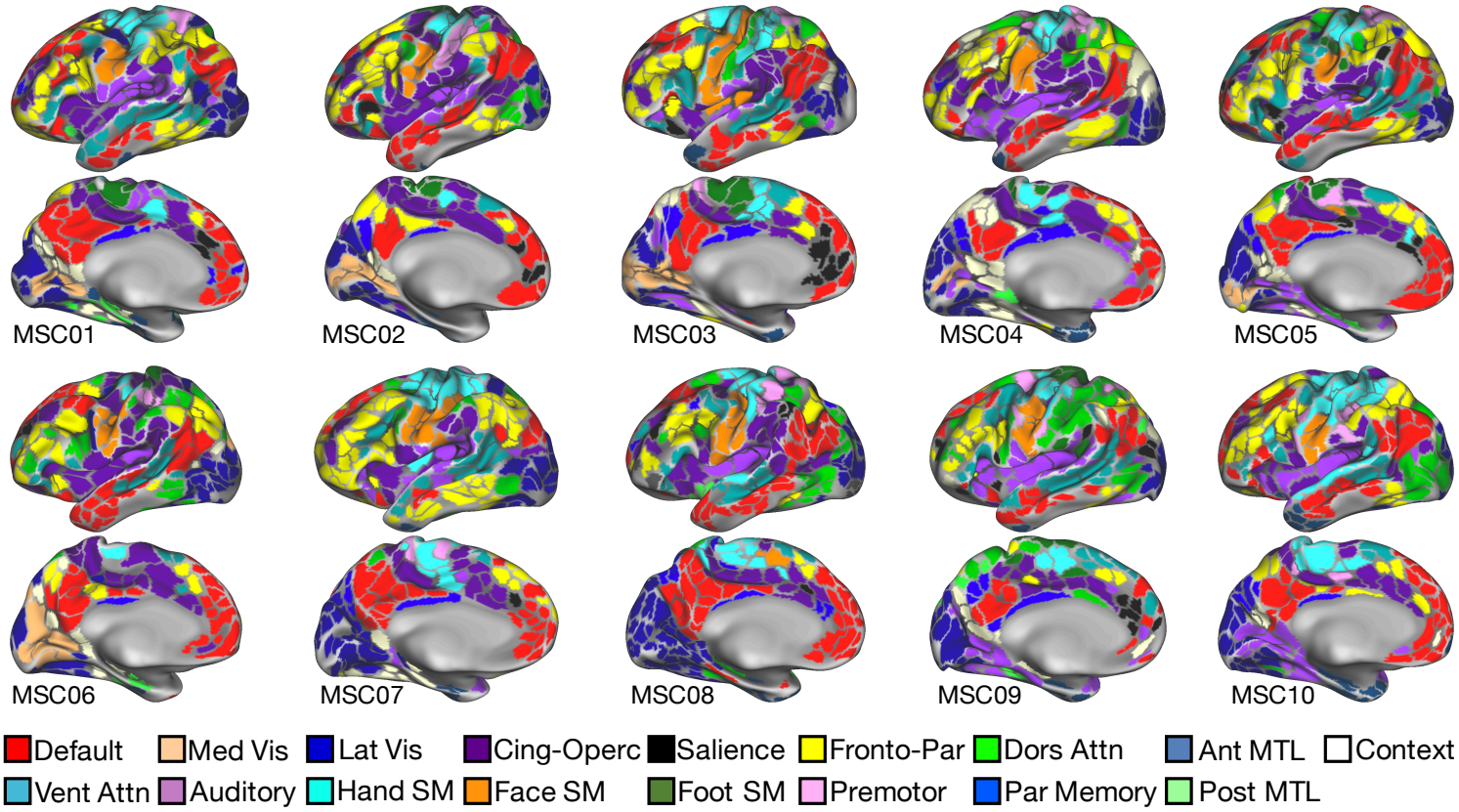

Figure S4. Related to Figure 4. Subject-specific parcellations and putative network identify of each parcel.

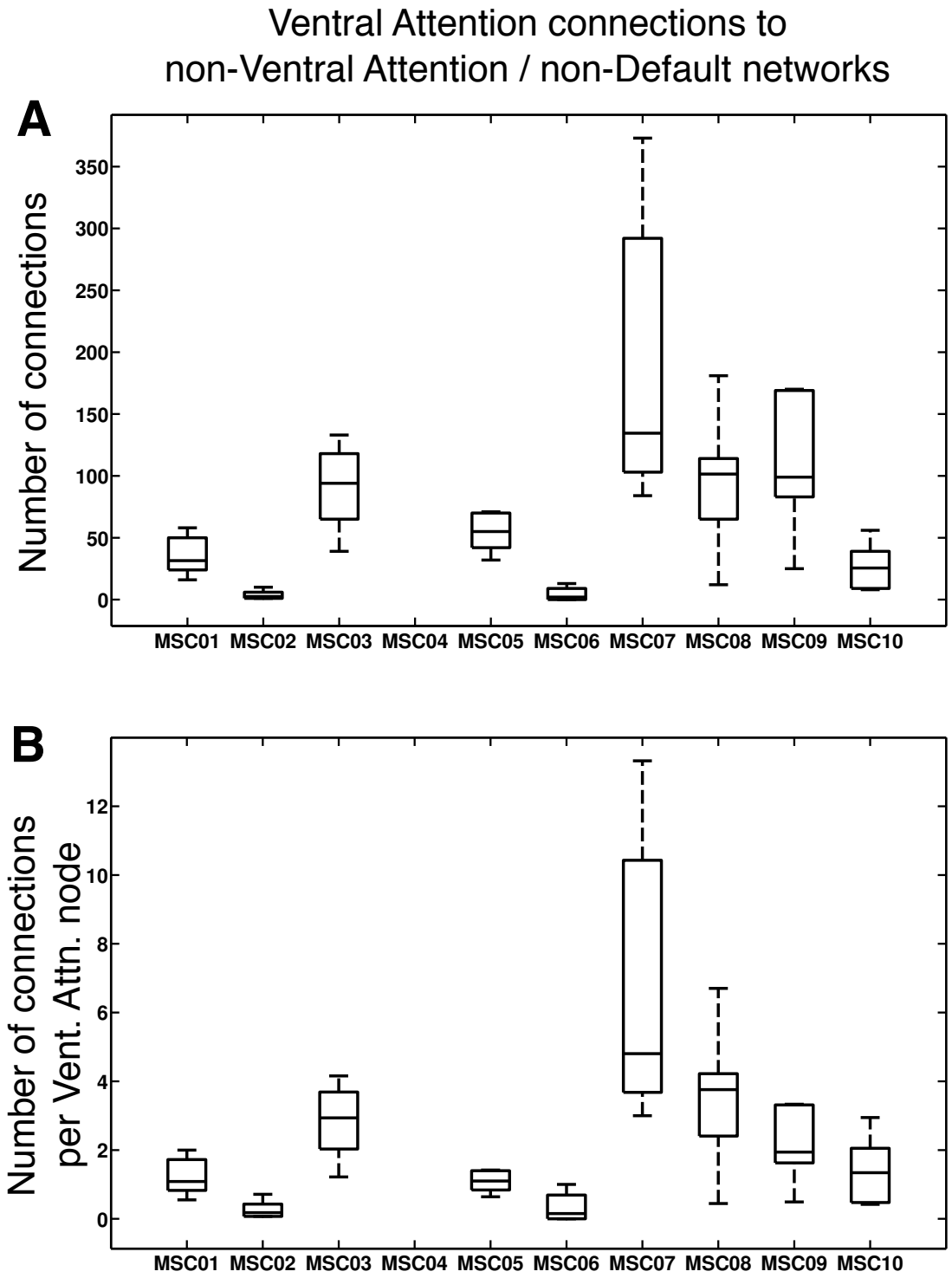

Figure S5. Related to Figure 4. Number of connections observed between the Ventral Attention network and regions outside the Ventral Attention / Default networks, at graph density = 2.5%. **A**: Across sessions, MSC Subjects 2 and 6 have fewer connections than all other subjects (all paired Ts(18) > 3.8, all ps < .001). **B**: These two subjects also have fewer connections per Ventral Attention node than all other subjects (all paired Ts(18) > 3.4, all ps < .005), indicating the effect is not driven by the size of the Ventral Attention network. Note that the Ventral Attention network could not be identified in MSC Subject 4.

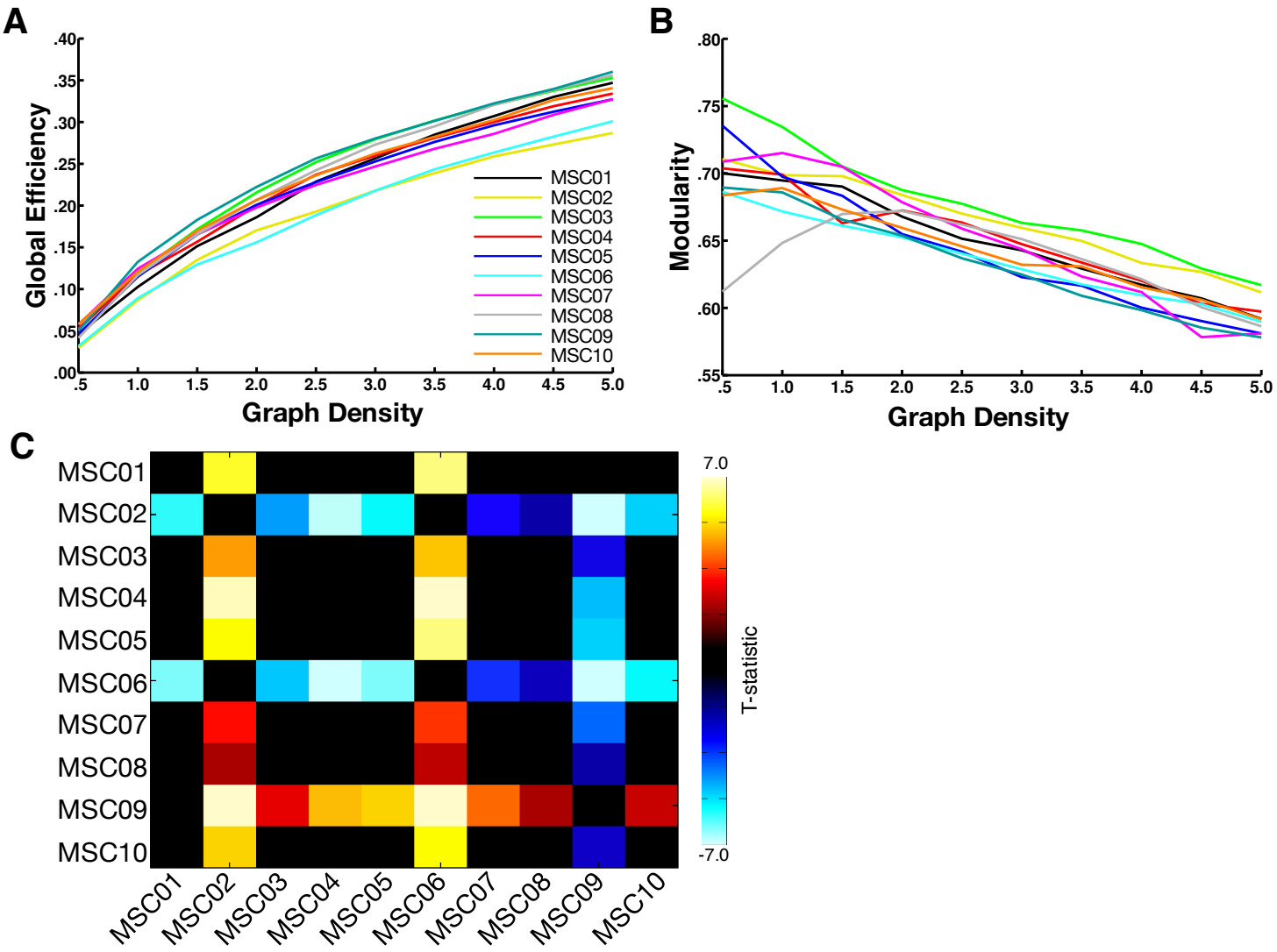

Figure S6. Related to Figure 4B. A: Global Efficiency values by density threshold. **B**: Modularity values by density threshold. **C**: Post-hoc pairwise comparisons of Global Efficiency (calculated at 2.5% density) between subjects. Significant ($p<.05$ uncorrected) pairwise differences between subjects are colored by T-score, with hot colors / positive values indicating the row-label subject had higher values than the column-labeled subject, and cool colors / negative values indicating the reverse.

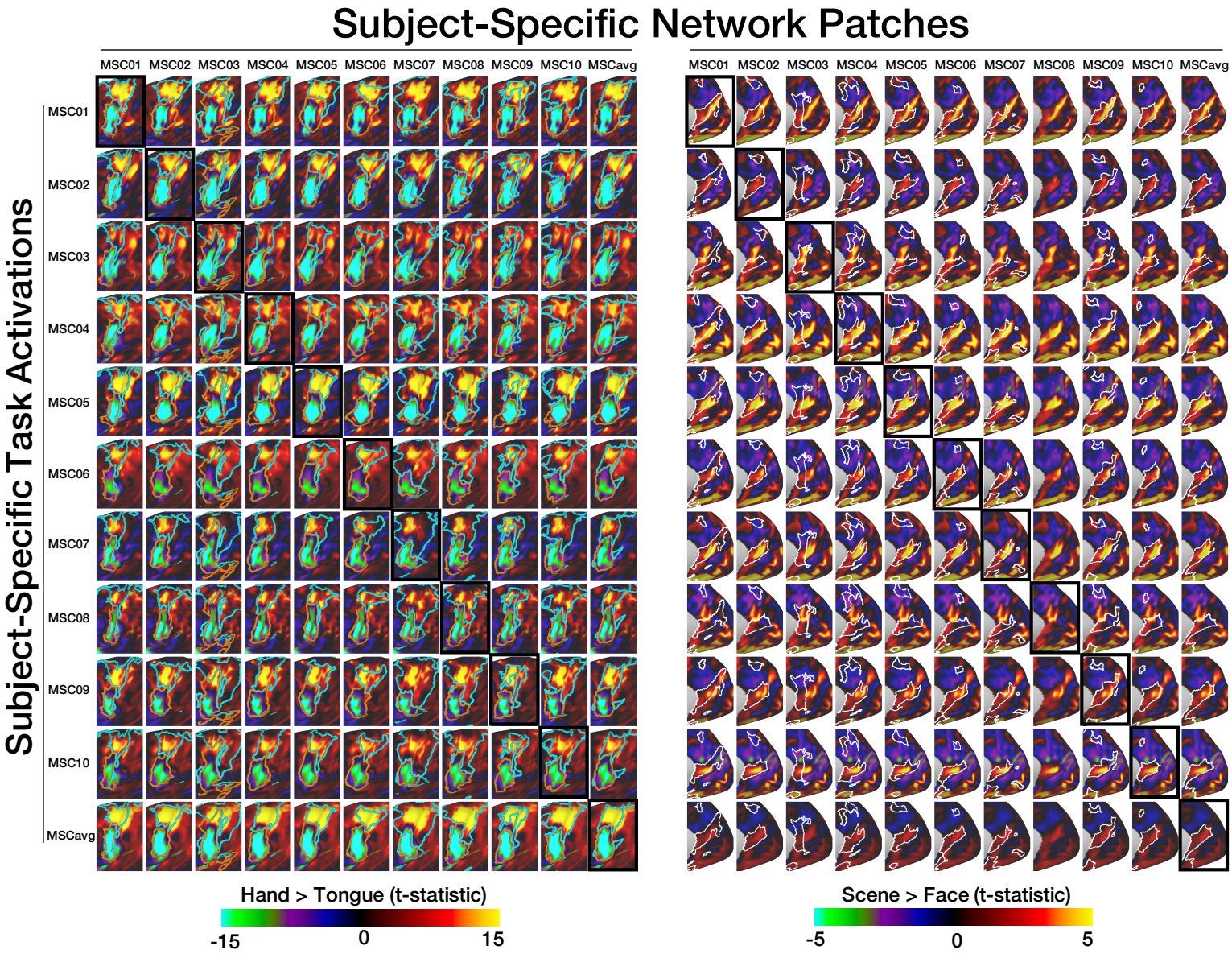

Figure S7. Related to Figure 6. Pairwise comparisons of all subject-specific and group-average task activation maps (rows) against all subject-specific and group-average RSFC-derived motor networks, as in Figure 6. Maps on the left side of the panel represent a hand > tongue task contrast, while maps on the right side represent a Scene > Face contrast. Boundaries of Somatomotor hand (cyan), Somatomotor face (orange), and Context (white) RSFC networks are shown on the surfaces.

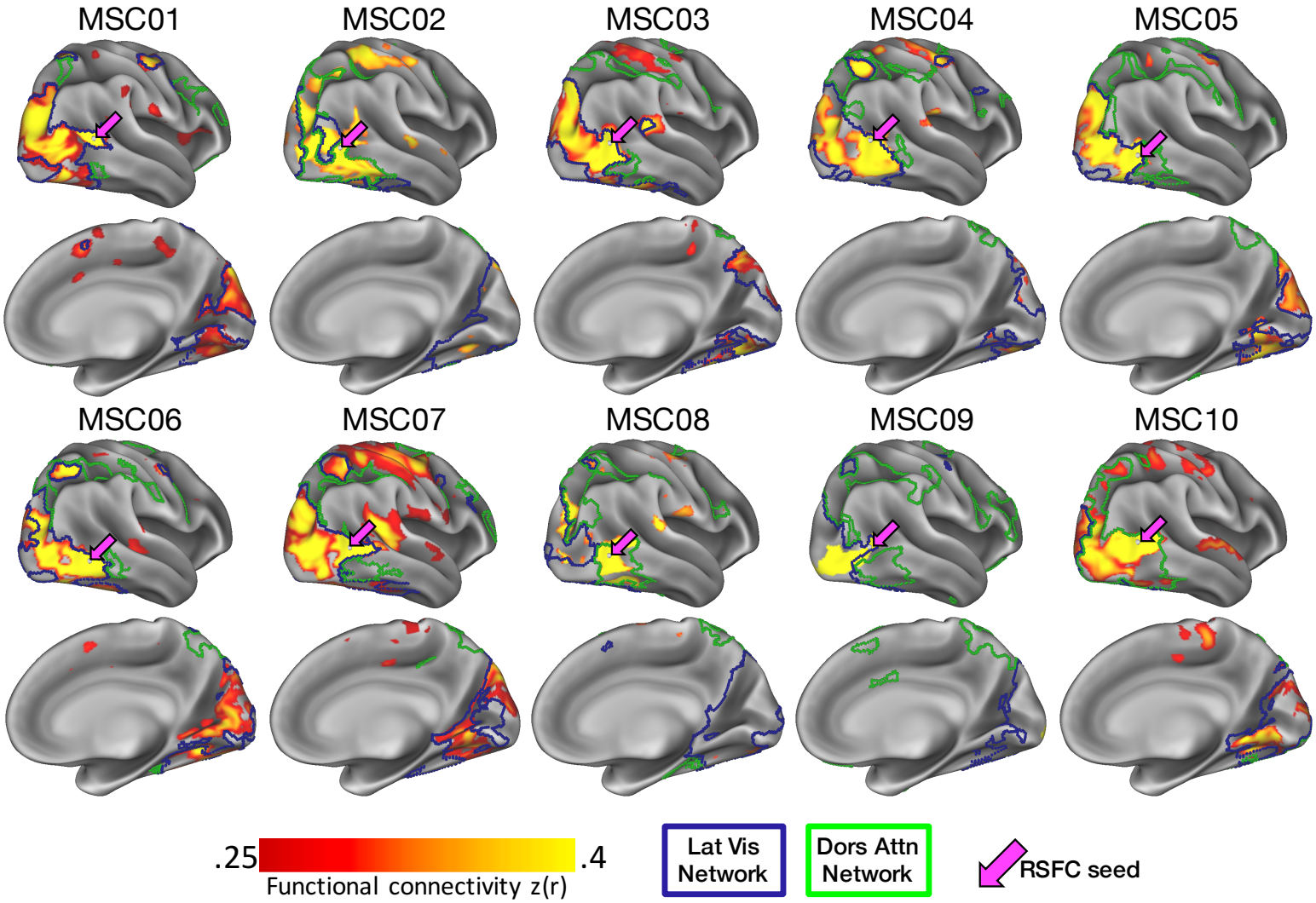

Figure S8. Related to Figure 7. Functional connectivity patterns seeded from putative right MT+ (magenta arrows), identified as the point in right lateral occipitotemporal cortex with maximal myelin content (see Figure 7). Maps display Fisher-transformed correlations representing the similarity of the MT+ timecourse with all other timecourses in the brain, thresholded at z(r) > .25. Blue and green borders represent the Visual 2 and Dorsal Attention networks, respectively. RSFC patterns can be observed to broadly respect the borders of the network containing the MT+ seed, and are almost never present across Visual 2 and Dorsal Attention network borders.

Table S1. Related to Figure 7. Talairach coordinates of putative MT+ regions in each subject, identified as the point in lateral occipitotemporal cortex with maximal myelin content (see Figure 7).

Subject	Hemisphere	Coordinates (Talairach)		
		x	y	z
MSC01	L	-45	-65	14
	R	41	-58	11
MSC02	L	-43	-70	13
	R	51	-65	8
MSC03	L	-46	-74	10
	R	39	-70	6
MSC04	L	-31	-76	5
	R	38	-70	11
MSC05	L	-39	-76	9
	R	40	-63	2
MSC06	L	-45	-64	-1
	R	39	-63	3
MSC07	L	-40	-71	10
	R	39	-65	0
MSC08	L	-39	-70	3
	R	41	-66	-1
MSC09	L	-34	-68	12
	R	39	-73	-1
MSC10	L	-43	-62	2
	R	42	-65	0